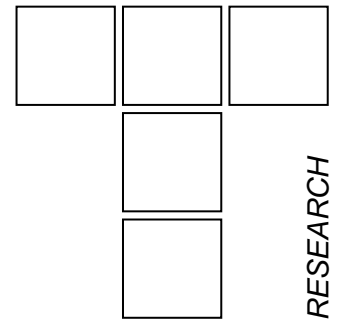


# Aspects of Analysis of Reverse Friction–Caused Contact Phenomena



*In the paper the contact phenomena caused by reverse friction “stick-slip” are discussed. To solve this complex problem, the authors have done the statistics, numerical computer simulation, bench tests as well as in-service tests on a real object. The paper presents the results of the numerical computer simulation. The effect of friction coefficient characteristics on how the wavy wear originates has been included. Keywords: numerical analysis, contact effect, reverse friction.*

**Keywords:** friction, stick-slip

## 1. INTRODUCTION

In the paper an assumption was made that during braking the friction processes between the wheel and brake insert are the main processes in the formation of wear in the contact area of these elements (Fig. 1).

The numerical analysis and experiments were done for wheel-brake shoe unit. The results were verified during in-service tests of rail-wheel-brake shoe unit on a real object.

## 2. NUMERICAL ANALYSIS OF BRAKE SHOE MOTION

Brake shoe motion has been simulated for a mechanical system shown in Fig. 2.

In the investigations it was assumed that in the analysis of the motion of the investigated system the translatory movement of the shoe is a basic motion, described by equation (6). The shoe rotational motion is assumed not to affect the motion of the investigated system and is thus disregarded in the present analysis.

From the analysis of the shoe motion shown in Fig. 2 it follows that a shoe of mass  $m$  supported by spring of springing rate  $c$  can move relative to the wheel rotating at the peripheral speed of  $v$ . In steady state, with no vibrations (Fig. 2b), the spring is extended by friction force  $F_N \mu(v)$  corresponding to speed  $v$ . This speed is then equal to relative speed of  $((v - \dot{x}))$ .



Figure 1. The wear area of the contact effect analysed by the authors

When the wheel drive is engaged or the spring is extra extended there appear vibrations - shoe motion relative to wheel (Fig. 2c).

In the conditions of stability these vibrations are damped and disappear. Thus the state shown in Fig. 2b becomes stable. However, self-excited vibrations can appear, due to the characteristics of friction between the shoe and wheel.

In case vibrations of the shoe appear, when its velocity at the given moment is  $\dot{x}$  (Fig. 2c), the relative velocity

$$v_r = v - \dot{x}, \quad (1)$$

will change in the neighbourhood of velocity  $v$ .

In the steady state (Fig. 2.b) the friction force (2)

---

Pawel PIEC, Cracow University of Technology,  
Cracow, Poland  
Stanisław PYTKO, University of Mining and  
Metallurgy, Cracow, Poland

$$T(v) = F_N \cdot \mu(v), \quad (2)$$

is equilibrated with force  $F_s$  of the spring (3)

$$F = c \cdot x_s. \quad (3)$$

So the shoe vibrations are affected by the difference of friction forces (4)

$$\Delta T = \Delta T(v) = T(v_r) - T(v). \quad (4)$$

During braking three various forms of shoe-wheel contact can be distinguished:

- a)  $\dot{x} = 0, \quad v > 0$  - shoe slip with no vibrations,
- b)  $\dot{x} \neq v, \quad v > 0$  - shoe slip following vibrations,
- c)  $\dot{x} = v, \quad v > 0$  - stick phase following stick-slip vibrations.

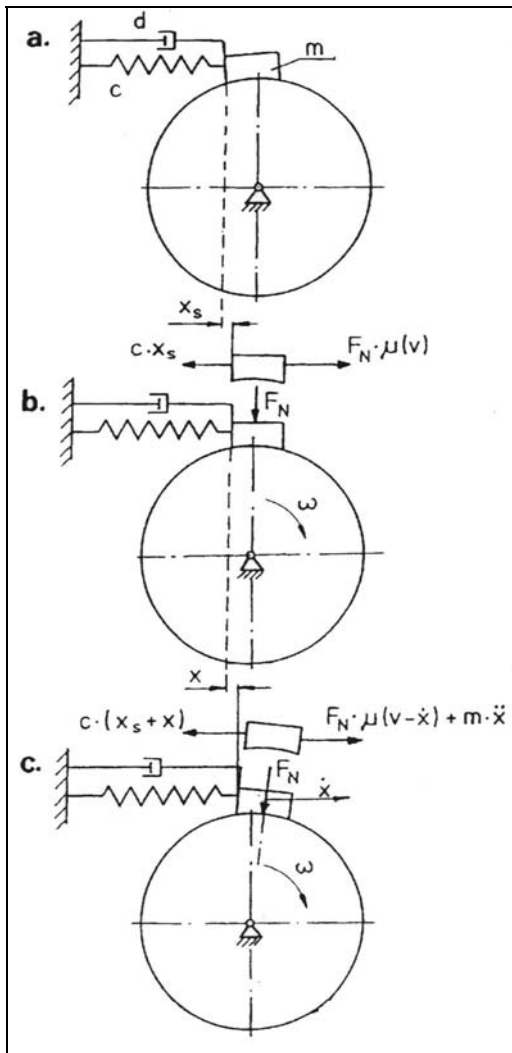


Figure 2. A diagram of the mechanical system under analysis:  $m$  – mass of brake shoe,  $c$  – elasticity constant,  $d$  – damping coefficient

The course of shoe-wheel interaction in which the stick and slip phases can be distinguished is called a boundary cycle. Fig. 3 shows the boundary cycle of

$R_{CG}$  radius. The shoe remains in the stick phase until the spring force is equal to the maximum friction force transferred. In this system the point of separation  $X_A$  can be calculated:

$$X_A = F_N \cdot \mu / c, \quad (5)$$

at which the shoe's stick phase changes into slip phase.

To describe the shoe motion mass  $m$  (Fig.2) differential equation of the second order is adopted (6):

$$m \cdot \ddot{x} + d \cdot \dot{x} + c \cdot x = \mu \cdot F_N \cdot \text{sgn}(\dot{x} - v), \quad (6)$$

where:

- $m$  – concentrated mass,
- $d$  – damping coefficient,
- $c$  – spring constant,
- $F_N$  - normal force.

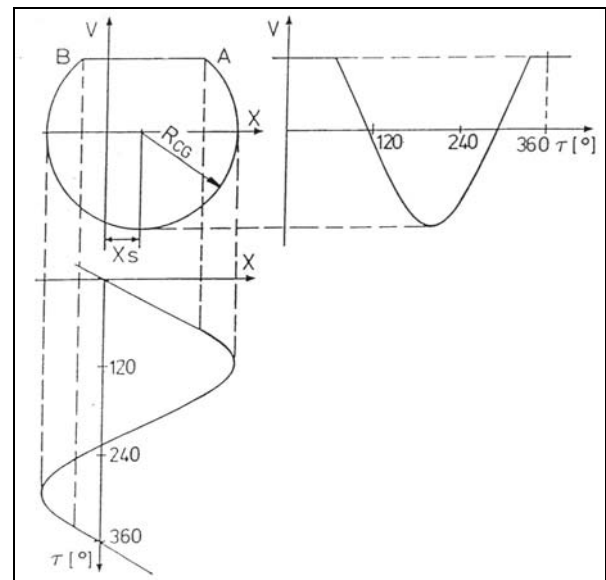


Figure 3. Diagram of boundary cycle of the investigated mechanical system

The wheel linear velocity  $v$  at the contact site with the shoe in this equation is discrete; it is hidden in the formula for friction coefficient.

It is convenient to run the analysis using dimensionless co-ordinates, which reduces the number of the system parameters. Hence (7)

$$\omega_o = \sqrt{\frac{c}{m}} \quad (7)$$

was introduced and a power unit was chosen. The choice helps to make the friction models uniform.

Introducing in equ. (6) the following:

non-dimensionless time

$$\tau = \omega_o \cdot t \quad (8)$$

non-dimensionless dislocation

$$X = \frac{c \cdot x}{F_N} \quad (9)$$

non-dimensionless damping coefficient

$$\gamma = \frac{d}{2 \cdot (c \cdot m)^{1/2}} \quad (10)$$

non-dimensionless velocity

$$V = \frac{v \cdot (c \cdot)^{1/2}}{F_N} \quad (11)$$

and coefficient

$$\delta = \frac{F_N \cdot \omega_0}{c} \quad \text{that is} \quad V = \frac{v}{\delta} \quad (12)$$

non-dimensionless friction coefficient

$$\mu \cdot \delta (X' - V) = \mu \cdot \delta \cdot (\dot{x} - v) / F_N \quad (13)$$

we get:

$$X'' + 2 \cdot \gamma \cdot X' + X = \mu \cdot \delta \cdot (X' - V) \cdot \text{sgn}(X' - V) \quad (14)$$

The parameters of equation (14) are:

- $\mu(V_r)$  - friction model,
- $\gamma$  - non-dimensional damping,
- $V$  - wheel non-dimensional velocity.

The programme for numerical simulation of stick-slip contact effects, i.e. shoe self-excited vibration has been written in PASCAL.

The numerical program presented defines an approximate solution of differential equation (6) which describes the shoe-wheel motion during braking at given initial conditions.

The input data for computer calculation program cover:

I. Characteristics of friction coefficient for the analysed materials of brake insert – representing the adopted friction models written as equations (15) and (16) for brake insert material “W<sub>1</sub>” (Fig.4) and equations (17) and (18) for brake insert material “Ws”, (Fig.5):

a). Friction model for brake insert material “W<sub>1</sub>”:

$$" \mu_s > \mu_k; \quad \mu_k = f(v) " \quad (15)$$

$$\mu(v_r) = \begin{cases} \mu_s & \text{for } v_r = 0, \\ \frac{\mu_s - \mu^*}{1 - \alpha |v_r|} + \mu_0 + \beta \cdot v_r^2 & \text{for } v_r \neq 0, \end{cases} \quad (16)$$

for:

$$\begin{aligned} \mu_s &= 0,4, \\ \mu^* &= 0,1, \\ \alpha &= 0,2 \text{ [s} \cdot \text{m}^{-1} \text{]}, \\ \beta &= 0.0 \text{ [s}^2 \cdot \text{m}^{-1} \text{]}, \text{ (Fig.4)} \end{aligned}$$

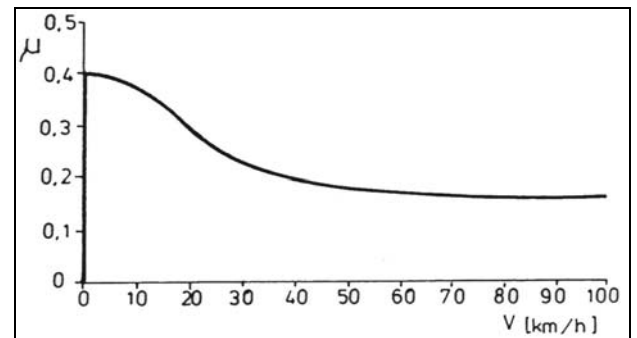


Figure 4. Model of friction - "  $\mu_s > \mu_k$ ;

$\mu_k = f(v)$ ", for brake insert material W<sub>1</sub>

b). Friction model for brake insert material “Ws”:

$$" \mu_s = \mu_k; \quad \mu_k = \text{const} " \quad (17)$$

$$\mu(v_r) = \begin{cases} \mu_s & \text{for } v_r = 0, \\ \mu_s & \text{for } v_r \neq 0, \end{cases} \quad (18)$$

for:  $\mu_s = 0,4$ , (Fig.5).

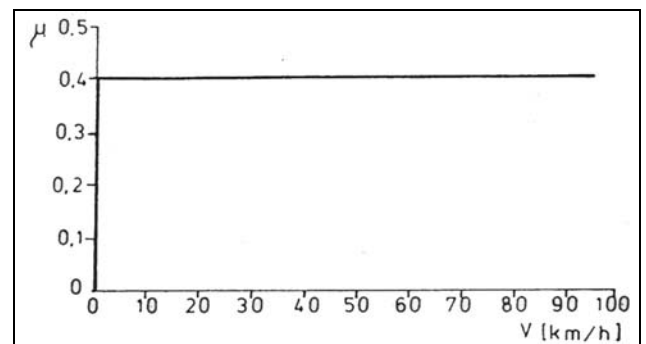


Figure 5. Friction model -

"  $\mu_s = \mu_k; \quad \mu_k = \text{const}$ ", for “Ws” brake insert material

The characteristics in “I” can be modified accordingly by the choice of kinetic friction

coefficient  $\mu_k$  and static coefficient  $\mu_s$ , as well as parameters  $\mu_*, \alpha, \beta, v_r$ .

II. Parameters of the investigated mechanical system, Fig. 2.

The parameters of the investigated mechanical system can be fed into calculations according to a given methodology of research as:

- values in dimensionless or dimensional coordinates and
- declared as values constant or variable in a given range, with calculation step defined.

### 3. RESULTS OF COMPUTER ANALYSIS

The friction model " $\mu_s > \mu_k; \mu_k = f(v)$ ", for brake insert material  $W_1$ , shows how the boundary cycle is formed (see Fig. 3).

At lower wheel velocities, for shoe initial speed  $X'_0 = 0$ , the unit approaches the boundary cycle (Fig. 6). At higher velocities there are observed only periodical vibrations with no boundary cycle; at further velocity increase a stable slip with no vibrations is observed.

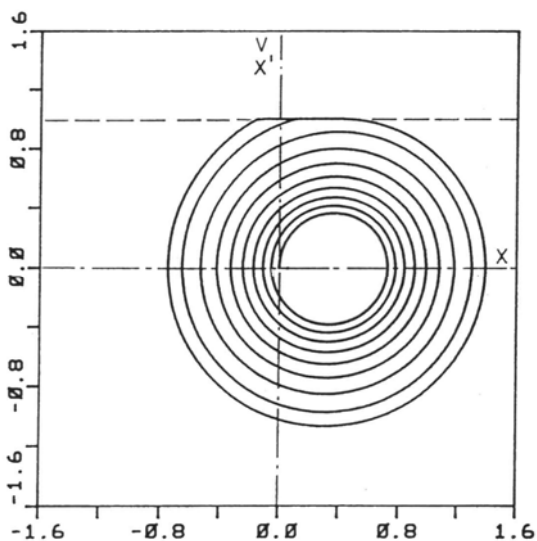


Figure 6. Phase diagram showing the behaviour of the unit during friction, for friction model

$$\begin{aligned} & \mu_s > \mu_k; \mu_k = f(v) \\ & (\text{insert material } W_1): V = 1, \\ & X_0 = 0, \gamma = 0, \delta = 1 \end{aligned}$$

The friction model " $\mu_s = \mu_k; \mu_k = \text{const}$ " for brake insert material  $W_s$ , unlike friction model " $\mu_s > \mu_k; \mu_k = f(v)$ " (brake insert material  $W_1$ ) does not cause the boundary cycle (see Fig.3).

Irregardless of the initial conditions, the unit shows only periodical vibrations without the boundary cycle, Fig.7.

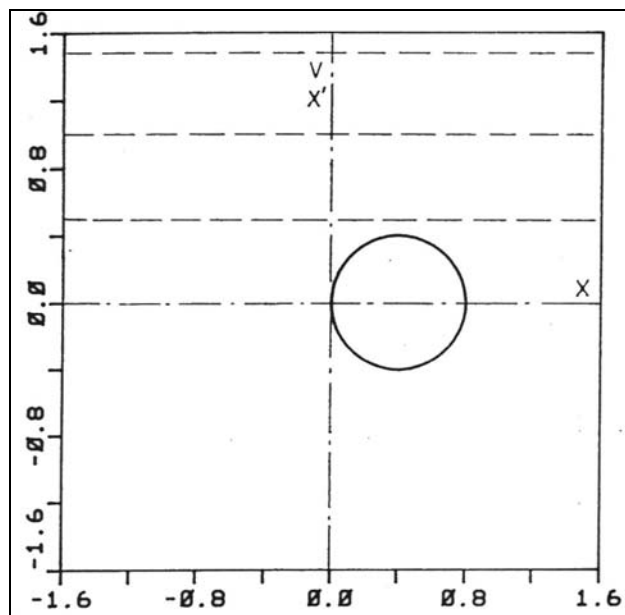


Figure 7. Phase diagram of the behaviour of the tested unit during friction, for friction model adopted

$$\begin{aligned} & \mu_s = \mu_k; \mu_k = \text{const} \\ & (\text{insert material } W_s): V = 0,5; 1; 1,5 \\ & X_0 = 0, \gamma = 0, \delta = 1 \end{aligned}$$

### 4. CONCLUSIONS

On the basis of the analysis of the results obtained in simulation of the effect of friction model " $\mu_s > \mu_k; \mu_k = f(v)$ " (insert material  $W_1$ ) on the behaviour of the mechanical system it was found that:

- at wheel lower velocities there occur stick-slip vibrations in the system;
- at higher velocities of the system there occur periodical with no boundary cycle.

On the basis of the analysis of simulation of the effect of friction model

" $\mu_s = \mu_k; \mu_k = \text{const}$ " (insert material  $W_s$ ) on the behaviour of the analysed mechanical system it was found that:

- irregardless of the initial conditions, there is no boundary cycle observed in the system.

### REFERENCES

- [1.] Piec P.: Zjawiska kontaktowe w elementach pojazdów szynowych. Wyd. ITE Radom, 1999.

[2.] Pytko S.: Problemy wytrzymałości kontaktowej. PWN, Warszawa 1982.

[3.] Uetz H.: Tribologie - Verschleisskunde. Vorlesungsmanuskript. Universitaet Stuttgart, 1980, Kpt.6, s.10